

## SPECTROPHOTOMETRY AND IMAGE ANALYSIS OF THE NEBULOSITY AROUND THE LOW-REDSHIFT QUASAR 0241 + 622

W. ROMANISHIN

University of California, Los Angeles

HOLLAND FORD<sup>1</sup>

University of California, Los Angeles; and Space Telescope Science Institute

ROBIN CIARDULLO

University of California, Los Angeles

AND

BRUCE MARGON<sup>1,2</sup>

Astronomy Department, University of Washington

Received 1983 January 17; accepted 1983 July 28

### ABSTRACT

We present digital imagery and spectrophotometry of the low-redshift QSO 0241 + 622. Video camera *B*, *V*, *R*, and *I* images taken with the KPNO 4 m telescope clearly show that 0241 + 622 is embedded in elliptical nebulosity. We analyze the pictures by comparing them to model images of a galaxy and central point source which were digitally convolved with a seeing point spread function. By varying the model parameters until the "smeared" image appears close to the observed image, we find that we can exclude the possibility that 0241 + 622 is the sum of a central point source and an elliptical galaxy. The 0241 + 622 pictures are well matched by the sum of a luminous disk galaxy and a central point source which is approximately twice as luminous as the galaxy. Spectroscopic observations of the nebulosity surrounding the quasar were obtained with the Lick 3 m and Kitt Peak 4 m telescopes. Although the spectra are not of sufficient quality to unambiguously detect individual absorption lines, the presence of a break in the spectrum at rest wavelength  $\lambda \sim 5300 \text{ \AA}$  suggests that the nebulosity contains stars. We conclude that 0241 + 622 is similar to several recently discovered low redshift quasars, and probably is a QSO-like nucleus in a spiral galaxy.

*Subject headings:* galaxies: structure — quasars — spectrophotometry

### I. INTRODUCTION

The object 0241 + 622 was discovered as the optical counterpart of a low galactic latitude 4U X-ray source (Apparao *et al.* 1978). Spectroscopic observations of 0241 + 622, reported by Apparao *et al.* and by Margon and Kwitter (1978, hereafter MK), showed that it has a quasar-like spectrum with a redshift of 0.0438. The object is heavily reddened by galactic absorption. The object 0241 + 622 appears stellar on the Palomar Sky Survey blue print and only slightly nonstellar on the Survey red print. Ford (1978) reported video camera observations which showed nebulosity around the quasar. Ford found that his *V* image could be roughly separated into a point source contribution and an exponential disk. Hutchings *et al.* (1982, hereafter HCCGM) included 0241 + 622 in a comprehensive radio and optical study of 29 QSOs. Their VLA observations resolved 0241 + 622 into a nuclear radio source and a second source which lies 4" E of the nucleus on the nebulosity's minor axis. Their *B* and *R* plates confirm the QSO's nebulosity and show that it declines exponentially along the major and minor axis.

In this paper, we discuss spectroscopy of the extended nebulosity surrounding 0241 + 622 and present a detailed

analysis of its optical image. We assume a Hubble constant of  $50 \text{ km s}^{-1} \text{ Mpc}^{-1}$  and  $q_0 = 0$ , which implies  $1'' = 1.27 \text{ kpc}$  and  $(m - M) = 37.14$  at 0241 + 622's redshift.

### II. IMAGING OBSERVATIONS AND ANALYSIS

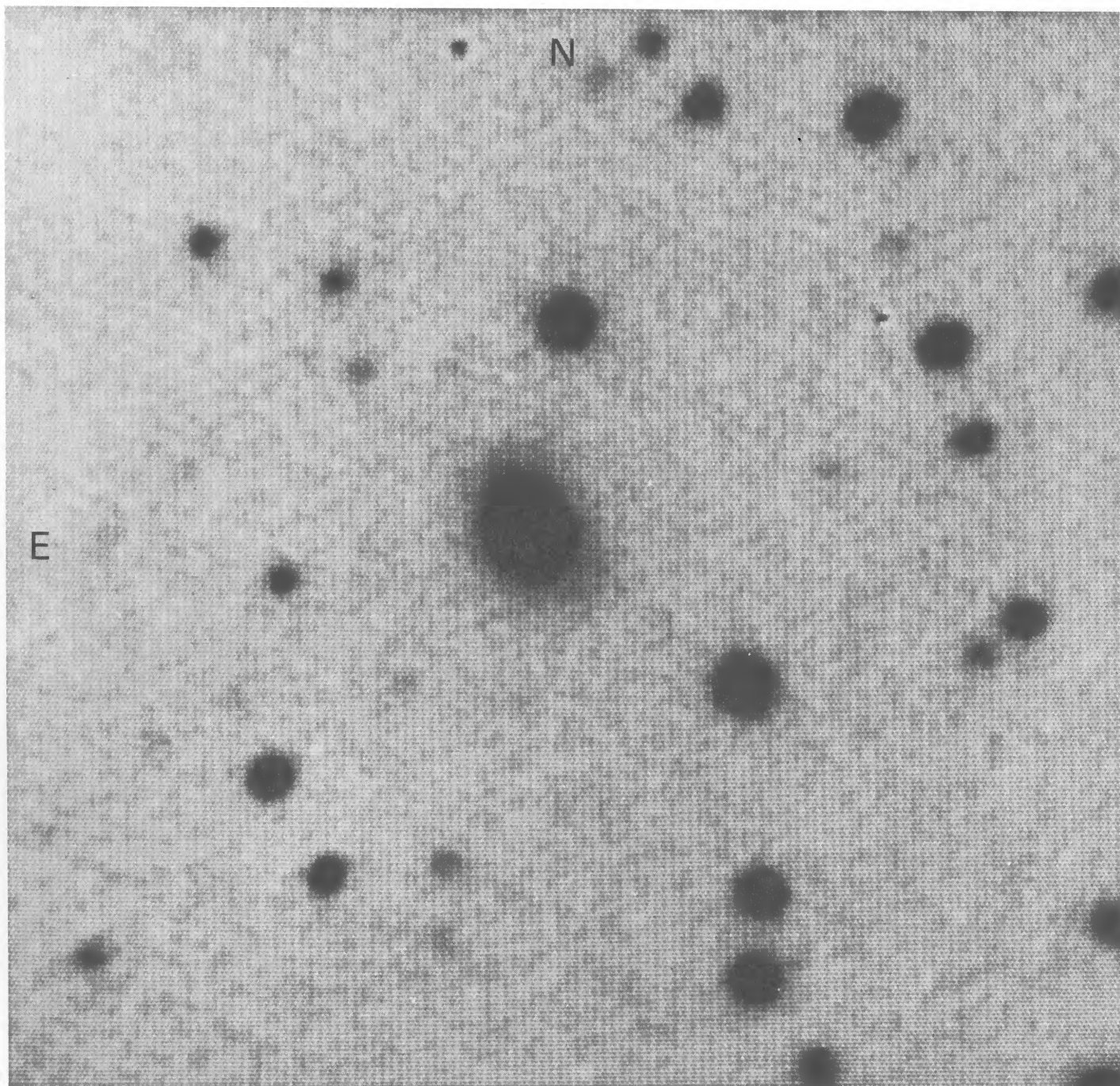
#### a) Observations and Data Reduction

Images of 0241 + 622 were obtained with the KPNO video camera and 4 m telescope on the night of 1977 December 6. Two 13.6 minute integrations were taken through a *V* passband, and one each through a *B* passband, an *R* passband, and an infrared passband, which we call *I*. The *I* filter combined with the detector response to give a passband from about 8300 to 8900  $\text{\AA}$ . Figure 1 shows the 4 m telescope *V* video camera image of 0241 + 622. With the exception of the *R* image, wherein 0241 + 622 was positioned in the corner of the video camera frame, the source was in the center of each picture. The nebulosity around the bright stellar source is progressively more apparent as the bandpass moves from blue to red.

The *V* images, which have the best signal-to-noise ratio (*S/N*) and cosmetic quality, were combined into a single image during the initial reduction. Before analyzing this frame, we compensated for a slight saturation in the central 1" by splicing on a stellar profile. The reduced *B* image contained an unexplained radially varying background. We removed this effect by dividing the image with an appropriately varying background. Because of this rather ad hoc treatment, we limited

<sup>1</sup> Visiting Astronomer, Kitt Peak National Observatory, which is operated by the Association of Universities for Research in Astronomy, Inc., under contract to the National Science Foundation.

<sup>2</sup> Alfred P. Sloan Foundation Research Fellow.



# VISUAL

FIG. 1.—A 13.6 minute *V* video camera image of 0241+622

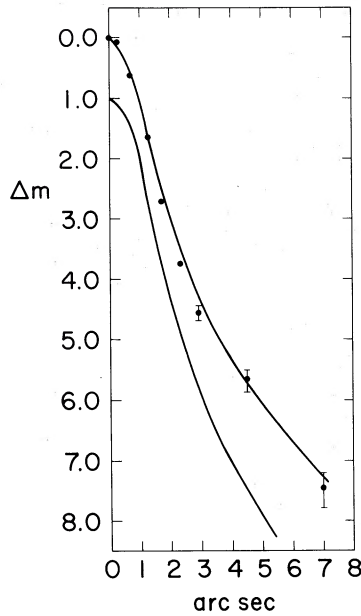


FIG. 2.—The  $B$  image profile of 0241+622 and the  $B$  point spread function (PSF). The filled circles are the observed profile of 0241+622. Error bars are shown only where the estimated error exceeds  $\pm 0.10$  mag. The solid line through the filled circles is the profile of the smeared Sa galaxy + point source model. The lower solid curve is the PSF.

our  $B$  profile to a  $7''$  radius, wherein the signal is at least 5 times the estimated sky uncertainty. Because of the high sky background and low detector sensitivity, the  $S/N$  of the  $I$  image beyond  $7''$  was too low for our analysis. Since the QSO was positioned near the edge of the  $R$  frame, we did not use this picture in our analysis.

We used observations of standard stars to transform the  $V$  image from instrumental to standard magnitudes. We did not derive a  $B$  calibration because of the peculiar problem affecting the sky background. Because no standard stars were observed in the  $I$  passband, we could not derive an  $I$  calibration. We derived a total  $V$  magnitude of 16.1 for 0241+622, with an uncertainty of 0.1 mag. This compares to 16.4 found by Margon and Kwitter (1978) using the Lick scanner. Because their measurement refers only to the central few arcsec of the image, the two measurements are consistent.

#### b) Analysis of the Image

We used the Kitt Peak Interactive Picture Processing System (IPPS) to measure the ellipticity, or  $b/a$  values, of the QSO image isophotes. In the  $V$  image,  $b/a$  was close to 1.00 near the center of the object, while at  $b = 10''$ ,  $b/a$  was 0.75. Our limiting value is consistent with the blue and red  $b/a$  ratios 0.61 ( $B$ ) and 0.70 ( $R$ ) measured by HCCGM at  $a = 6''$ .

We measured the azimuthally averaged QSO image luminosity profile with standard IPPS software, which is briefly described in Strom and Strom (1978). We obtained luminosity profiles by averaging intensity values in  $0''.25$  radius circular apertures spaced along elliptical isophotes. The semiminor axes of the concentric ellipses were separated by  $0''.5$ . The resulting luminosity profiles and the shape of the point spread function are shown in Figures 2–4. The error bars represent uncertainty estimates from two sources: (1) uncertainty in the sky intensity level, and (2) uncertainty in the signal at a given radius.

We assume that the 0241+622 image results from atmospheric smearing of an unresolved source (the QSO) and an underlying galaxy. We constructed two-dimensional digital “images” by first adding a galaxy luminosity distribution to a central point source, and then convolving the resultant intensity matrix with a digital point spread function (PSF). The PSF was derived from stellar luminosity profiles in the same frame as 0241+622. By varying the parameters of the underlying model galaxy, and the ratio of point source to total galaxy luminosity, we searched for reasonable combinations of parameters which reproduce the observed luminosity distribution. Although we will not find a unique representation using this technique, our approach does serve to answer two important questions about the QSO image: (1) Can the luminosity profile be understood as the sum of a point source plus some type of normal galaxy? (2) If so, can we determine or constrain the morphological type of the underlying galaxy?

We used three model galaxy luminosity profiles: (1) pure elliptical, (2) pure disk, and (3) a combination of disk plus elliptical (i.e., nuclear bulge) with parameters chosen to represent an Sa spiral. For the elliptical, we assumed a de Vaucouleurs luminosity law, where  $I(r)$ , the intensity as a function of radius, is represented by:

$$\log [I(r)/I_e] = -3.33[(r/r_e)^{1/4} - 1]. \quad (1)$$

The effective radius,  $r_e$ , is the radius containing half the total light, and  $I_e$  is the intensity at  $r_e$ . We used an exponential intensity profile for the pure disk galaxy:

$$I(r) = I_0 \exp(-\alpha r), \quad (2)$$

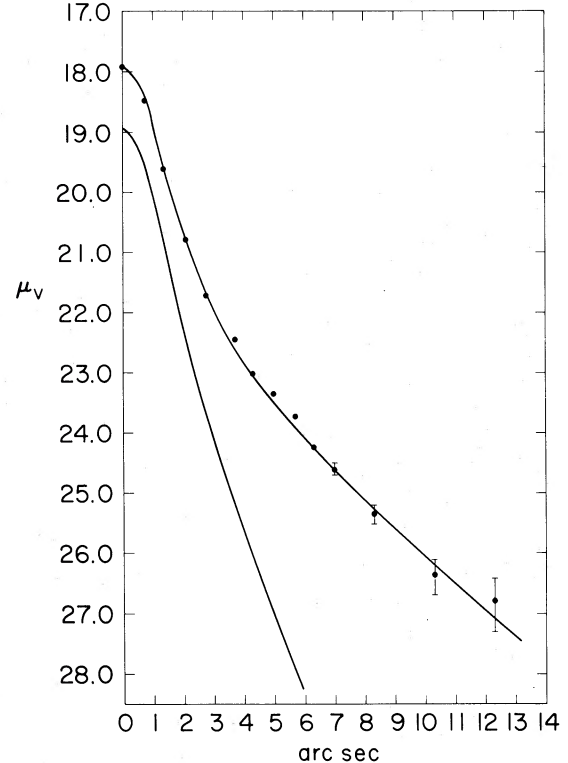


FIG. 3.—The  $V$  image profile of 0241+622 and the  $V$  PSF. The units of the ordinate are  $\text{mag arcsec}^{-2}$ .

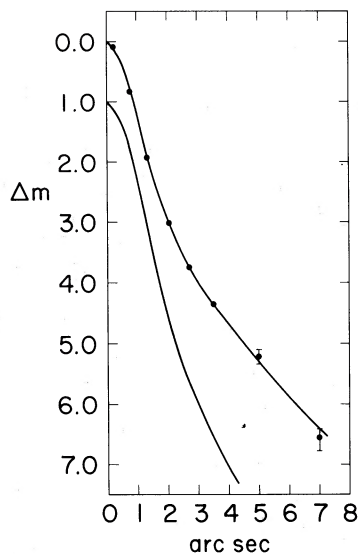


FIG. 4.—The  $I$  image profile of 0241+622 and the  $I$  PSF

where  $\alpha^{-1}$  is the disk scale length and  $I_0$  is the intensity at  $r = 0$ . For the combination disk plus elliptical, the profile is fixed by specifying  $\alpha^{-1}$ , the ratio  $r_e/\alpha^{-1}$ , the ratio of the bulge (elliptical) to disk luminosity ( $B/D$ ), and the total galaxy luminosity. Observed spirals vary widely in  $B/D$  and  $r_e/\alpha^{-1}$ , even at constant Hubble type. Our combination model has  $r_e/\alpha^{-1} = 0.4$  and  $B/D = 0.9$ , appropriate for average Sa galaxies (Borson 1981). For the calculation of inclined disk models, we assumed the disk was a transparent plane, with an exponential intensity falloff within the plane.

The effects of atmospheric smearing were modeled by representing the PSF as a  $19 \times 19$  pixel matrix with  $1''$  spacing. Model galaxies with sizes equal to or larger than  $50 \times 50$  pixels (large enough to avoid edge effects) were then convolved with this PSF. After smearing the galaxy plus QSO image, the major axis luminosity profile was extracted, converted to magnitudes relative to  $r = 0$  and normalized at  $r = 0$  to the observed profile. After calculating the residuals ( $I_{\text{observed}} - I_{\text{smearred}}$ ), the model parameters were modified to produce a better fit. An “adequate” fit for the  $V$  profile was defined as one in which the maximum residual did not exceed 0.15 mag at radii less than  $10''$ , beyond which residuals up to 0.5 mag were tolerated because of the increasing uncertainty in the observed profile. The best fits had a mean residual of 0.02 mag or less, and a dispersion of less than 0.1 mag.

Like Ford (1978), we found that no model of an elliptical plus point source would provide a reasonable fit to the data. All elliptical models which had enough light in the outer parts of the profile ( $7''$ – $10''$ ) had too much light at radii around  $5''$  to agree with the observed profile. The satisfactory fits obtained with the Sa and pure disk models strongly suggest that the underlying nebulousity is a disk galaxy. In Table 1 we list the ratio of point source flux [ $F(\text{pt})$ ] to total galaxy flux [ $F(\text{gal})$ ] in each color for the best two models.

The uncertainty in  $F(\text{pt})/F(\text{gal})$  was estimated by varying this ratio until the fit was clearly unacceptable. The estimated uncertainty in  $B$  and  $I$  is  $\pm 20\%$ , while for  $V$  it is  $\pm 10\%$ . In all

TABLE 1  
RATIO OF POINT SOURCE FLUX TO  
TOTAL GALAXY FLUX:  $F(\text{pt})/F(\text{gal})$

Model	$B$	$V$	$I$
Sa .....	3.5	2.0	1.5
Disk .....	6.0	3.3	2.5

these models,  $\alpha^{-1}$  was  $2''.2$  (2.8 kpc), a value found by trial and error fitting the  $V$  profile. Our scale length is in excellent agreement with HCCGM ( $2''.2$  blue and  $1''.6$  red). The Sa model fit is shown as the upper solid line in Figures 2–4. We find equally adequate fits for both the Sa and pure disk galaxies because the bulge of the Sa model, which has an effective radius of only  $1''.1$ , approximates a point source. The final model galaxies had a disk with  $b/a$  of 0.75. The resulting smeared image had a run of  $b/a$  with radius similar to that of the observed image.

### c) Reddening

The problem in comparing the derived galaxy parameters with those of other galaxies is the large and uncertain galactic extinction in the direction of 0241+622. MK used several independent but individually uncertain arguments to arrive at an estimate of  $E(B-V) = 1.4$  for 0241+622. If the central object has a power-law continuum and the underlying object has the spectral energy distribution of a normal galaxy, we can derive a reddening estimate using a modification of the intrinsic power law slope method used by MK. Since the ratio of  $F(\text{pt})/F(\text{gal})$  between two colors determines the color difference, or relative spectral slope between the point source and galaxy, the assumption of a known energy distribution for the underlying galaxy yields the intrinsic slope of the central source. Once we have this intrinsic slope we can find the reddening, using the table of reddening versus intrinsic slope presented by MK.

One problem with this method is that emission lines may appear in a filter bandpass. We made a slight correction for the  $H\beta$  and  $[\text{O III}]$  lines, which fall in the  $V$  filter. No correction was needed in the  $B$  or  $I$  filters.

Because the spectral energy distribution of the underlying galaxy is uncertain, we adopted several different standard spectral energy distributions (Pence 1976). Table 2 lists the central point source slope between the  $V$  and  $I$  bands (approximately 5200–8200 Å in the object rest frame) for each galaxy type and the corresponding  $E(B-V)$  value derived from interpolation in MK’s table. We also derived the slopes between

TABLE 2  
ASSUMED GALAXY TYPE VERSUS INFERRED  
INTRINSIC QUASAR CONTINUUM SLOPE

Galaxy Type	Inferred Continuum Slope	Inferred $E(B-V)$
E/SO .....	1.5	0.8
Sab .....	1.6	0.8
Sbc .....	0.7	1.1
Scd .....	0.0	1.3

TABLE 3  
INFERRED GALAXY PARAMETERS

$E(B-V)$	$M_{V(\text{pt})}$	$M_{V(\text{gal})}$	$B(0)_c$
0.6 .....	-22.5	-21.8	20.6
0.8 .....	-23.2	-22.5	20.0
1.0 .....	-23.9	-23.1	19.3
1.2 .....	-24.5	-23.8	18.7
1.4 .....	-25.2	-24.4	18.0

the  $B$  and  $I$  passbands (approximately 4200–8200 Å in the rest frame of 0241+622). These slopes are about 0.2 lower than the  $V-I$  slopes. We list the 5200–8200 Å slopes because this range best matches the 5000–7000 Å range considered by MK. It is possible that in our  $B$  passband the spectrum of the central source rises above the power-law slope extrapolated from larger wavelengths, due to emission related to the “3000 Å bump” (Grandi 1982; Malkan and Sargent 1982). We estimated the uncertainty in the slope by assuming that the only errors are in the previously discussed values of  $F(\text{pt})/F(\text{gal})$ . This gives an uncertainty of  $\pm 0.3$  for the slopes, which corresponds to a  $\pm 0.1$  uncertainty in the respective  $E(B-V)$  values.

#### d) Galaxy Parameters

Table 3 displays the absolute visual magnitude of the point source and galaxy for various values of  $E(B-V)$ , assuming  $A_V = 3.3 \times E(B-V)$  and the Sa model for the galaxy. If the pure disk galaxy were used, the galaxy magnitudes would be about 0.4 mag fainter and the point source about 0.1 mag brighter. Also listed in Table 3 are values of  $B(0)_c$  for the Sa model, assuming  $(B-V) = 0.8$  for the intrinsic color of the galaxy disk. For the pure disk galaxy,  $B(0)_c$  would be about 0.3 mag brighter.

A reddening as large as that suggested by MK,  $E(B-V) = 1.4$ , requires that the 0241+622 galaxy be blue, with the color of a late spiral, and extremely luminous ( $M_V = -24.4$ ). Spirals this luminous exist (Romanishin 1983) but are very rare. A much more plausible reddening is  $E(B-V) = 1.0$  or less, implying a spiral galaxy with  $-22 > M_V > -23$  and an early-to-middle-type spectral energy distribution.

Can the surface brightness or disk scale length be used to put constraints on the underlying galaxy? If the reddening is as large as suggested by MK, the central  $B$  surface brightness of the exponential disk is around 18.0. Boroson's data show that the distribution of blue central surface brightnesses for normal spiral galaxies peaks between 21 and 22, but that the distribution is fairly broad. Because of the large dispersion of  $B(0)_c$  values, we cannot definitely rule out a galaxy with  $B(0)_c = 18$ , although they must be rare. The disk scale length for the model galaxy falls towards the low end of the distribution for normal spiral galaxies (see Boroson 1981). Unfortunately, as disk scale lengths are available for only a handful of galaxies, nothing is known about any possible systematic behavior of disk scale length with galaxy luminosity.

Because of the variation in normal spirals, we cannot use the underlying galaxy's luminosity, scale length, or central surface brightness to put firm constraints on the 0241+622's reddening. However, it is apparent that the galaxy parameters become much more plausible with a value of reddening lower than that suggested by MK.

### III. SPECTROSCOPY

Spectrophotometry of the 0241+622 nebosity can in principle reveal whether the light comes from an underlying galaxy, ionized gas, or some other source. Because the nebosity is much fainter than the central nonthermal source, we made spectrophotometric observations with occulting apertures which blocked the quasar-like light. At Lick Observatory we observed 0241+622 with the Image Tube Scanner (ITS; Robinson and Wampler 1972, 1973) at the Cassegrain focus of the Shane 3 m telescope through an annular aperture with radii of 3" and 5". Because of the circular aperture's relatively poor spectral resolution and the fact that the nebosity is clearly elongated at a position angle of 35° (cf. Fig. 1), we reobserved 0241+622 at Kitt Peak with the Intensified Image Dissector Scanner (IIDS) on the 4 m telescope through a pair of 2" × 4" rectangular apertures separated by 4".9. The position angle of the apertures was rotated to coincide with the position angle of the nebosity. At both Lick and Kitt Peak we used television acquisition systems to keep the QSO image centered on the aperture's occulting disk or bridge. These observations are summarized in Table 4.

TABLE 4  
SPECTROSCOPIC OBSERVATIONS OF 0241+622

Object	UT Date (1978)	Integration Time (min)	Grating (lines mm <sup>-1</sup> λ blaze)	λ Central (Å)	Aperture
Lick Observatory 3 m Telescope ITS					
Nebulosity .....	Sep 30	200	600/5000	5250	3"-5" annulus
Nucleus .....	Sep 30	16	600/5000	5250	3"-5" annulus
Nebulosity .....	Oct 1	200	600/5000	5250	3"-5" annulus
Nucleus .....	Oct 1	12	600/5000	5250	3"-5" annulus
Kitt Peak 4 m Telescope IIDS					
Nebulosity .....	Nov 1	92	500/5000	5320	2" × 4" paired
Nebulosity .....	Nov 2	152	500/5000	5320	2" × 4" paired
Nucleus .....	Nov 2	12	500/5000	5320	2" × 4" paired

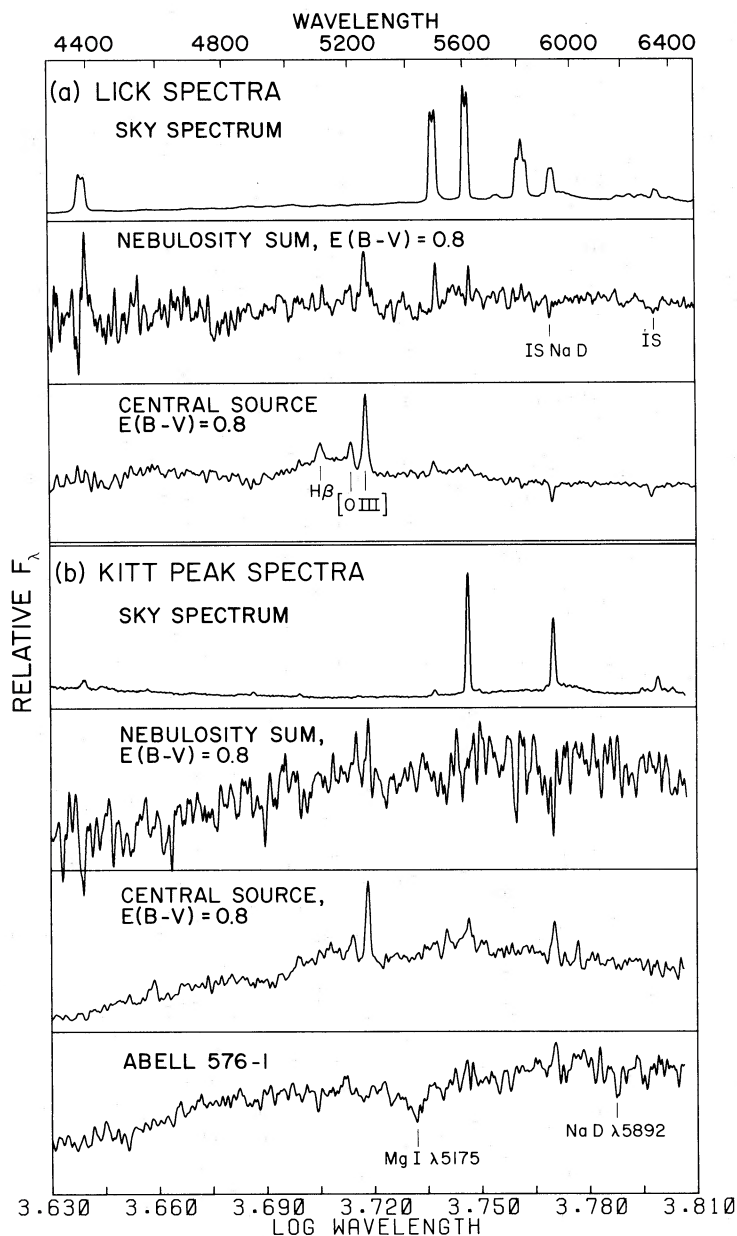


FIG. 5.—Spectra of 0241 + 622 and its surrounding nebula. The double-peaked line profiles in the Lick data are due to the poor resolution and the circular geometry of the occulting aperture. The fluxes are plotted against the logarithm of wavelength for easy comparison with the spectrum of Abell 576-1, a bright, early-type galaxy at  $z = 0.044$  (Peterson 1970; Sandage 1972).

We removed pixel-to-pixel detector irregularities by dividing the raw data by a continuum lamp spectrum taken at the beginning and ending of each night. Wavelength calibrations for the scans were determined from fifth-order polynomial least squares fits to comparison lamp spectra obtained at the QSO's telescope setting. The effects of atmospheric extinction were removed by using the mean extinction coefficients for Mount Hamilton and Kitt Peak. The scans were reduced to relative flux by using instrument response curves derived from observations of standard stars (Stone 1974, 1977; Oke 1974).

The Lick and Kitt Peak 0241 + 622 spectra are shown in Figures 5a and 5b. Each panel shows a sky spectrum, the sum

of two nights' observations of the nebula, and a spectrum of the central nonthermal source, all smoothed with a Gaussian function (FWHM = 2.5 channels). The sky spectra are displayed to provide a measure of the resolution through the occulting apertures and to show the wavelengths at which imperfect sky subtraction may introduce artificial spectral features. The scans in Figure 5 are plotted on a logarithmic wavelength scale in order to facilitate intercomparison of spectra which may originate at different redshifts. We used Whitford's (1958) reddening curve to rectify the spectra with our best estimate of the interstellar reddening,  $E(B-V) = 0.8$ .

A reference spectrum of an early-type galaxy observed on

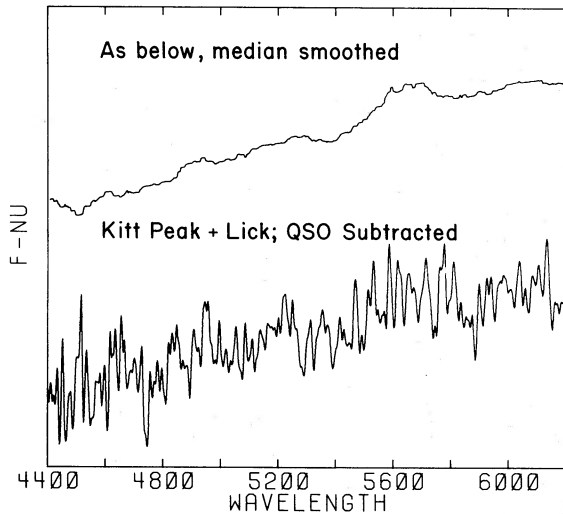


FIG. 6.—The bottom spectrum is the sum of the Lick and Kitt Peak scans of 0241+622's nebulosity corrected for QSO light contamination and dereddened by  $E(B-V) = 0.8$ . The top spectrum is the result of smoothing the bottom spectrum with a 103 channel median smoothing function. Although virtually all of the noise and possible spectral lines have been smoothed away, the continuum break at  $\lambda \sim 5300$  Å is now obvious.

the same night and in the same instrumental configuration as the QSO is shown at the bottom of Figure 5b. This galaxy, one of the brightest members in the cluster Abell 576, was chosen because its redshift ( $z = 0.042$ ) is close to the emission-line redshift of 0241+622 ( $z = 0.044$ ).

Comparison of the spectra shows that our Lick and Kitt Peak observations are contaminated by scattered light from the central nonthermal source. [O III]  $\lambda 5007$ , presumably originating in the QSO, is visible in both nebulosity spectra. Shortward of 5200 Å, the energy distribution of the nebulosity appears to follow that of the central source. This effect is much more pronounced in the Lick data than in the Kitt Peak data. We attribute this to the less favorable geometry of the Lick occulting aperture. Both nebulosity spectra, however, rise faster than the spectrum of the central source longward of 5200 Å, indicating that the nebulosity continuum radiation is redder than the QSO. We also note that the QSO continuum is considerably bluer in the Lick scans than in the Kitt Peak scans. One explanation is that the scans have been affected by atmospheric dispersion. However, the image elongation in our spectral bandpass (0".45 at Lick and 0".8 at Kitt Peak) probably was too small relative to the apertures (2" and 3") to explain the difference. Although we cannot account for the difference, we think it does not affect the subsequent analysis.

In order to study the spectrum of the nebulosity, we removed, as best we could, the contamination caused by the central source. This was done by incrementally subtracting the emission-line spectrum of the central source from the spectrum of the nebulosity until the [O III]  $\lambda 5007$  line largely disappeared. This procedure may have overestimated the QSO contribution, as some [O III] emission may originate in the nebulosity. We then combined the Lick and Kitt Peak data to form the grand sum nebulosity spectrum appearing in the bottom panel of Figure 6. This spectrum exhibits some features which might be absorption lines. The feature at 5395 Å could correspond to

Mg I  $\lambda 5175$  at  $z = 0.044$ . However, other characteristic absorption features are not identifiable at this redshift.

The signal-to-noise ratio in the nebulosity spectra is apparently not sufficient to unambiguously detect individual absorption lines, if they are indeed present. Another spectral signature of starlight is the presence of spectral breaks, or relatively sharp changes in the average flux level. The most prominent is the 4000 Å break (Spinrad 1976). Another break, possibly useful in interpreting the 0241+622 nebulosity spectrum, appears at 5280 Å. This break is easily seen in the spectrum of the nucleus of the galaxy VII Zw 421 (Sparke, Kormendy and Spinrad 1980) and in spectra of galaxies 2 and 3 presented by Phillips (1980).

We examined the nebulosity spectrum for this break by converting the data to  $F_V$  and then smoothing it with a 103 channel median filter. The median filter has the advantage of allowing extensive smoothing without smearing edges or discontinuities as much as other smoothing routines (Justusson 1981). The median smoothed spectrum is shown in the top section of Figure 6. If the break visible at 5500 Å in the nebulosity spectrum is identified as the 5280 Å discontinuity, the redshift is 0.042. The amplitude of the break is consistent with the break in VII Zw 421.

The presence of the 5280 Å break at approximately the same redshift as the QSO suggests that the nebulosity is a galaxy. As discussed above, our procedure may have overestimated the QSO contribution to the nebulosity spectrum. However, a median smoothed plot of the nebulosity spectrum with no QSO contribution subtracted shows the break at a similar level.

#### IV. DISCUSSION

The spectroscopic and imaging observations presented here provide evidence that 0241+622 is a very luminous source located in the nucleus of a disk galaxy. Our observations add to the growing body of data that some QSOs occur in galaxies with disks. The largest and most homogeneous set of observations are the 29 low-redshift QSOs studied by HCCGM. Their three lowest redshift QSOs, which include 0241+622, have indistinguishable exponential profiles, and in their best data among the remaining QSOs, an exponential decline provides a better fit to the underlying nebulosity than an  $R^{-1/4}$  decline. Bothun *et al.* (1982) showed that the X-ray-selected QSO 0351+026 appears to be in a low-luminosity spiral which has an interacting companion, a conclusion supported by HCCGM. ESO 113-IG45 (West, Danks, and Alcaino 1978) and IC 4329A (Wilson and Penston 1979) are two low-redshift spirals which have nuclei with QSO-like luminosities and spectra. If these two galaxies were heavily reddened, they would appear similar to 0241+622. If they were considerably further away the underlying disks would be undetectable, or would appear only as faint nebulosity around the bright center (a conclusion stressed by Bothun *et al.* 1980).

The properties of low-redshift QSOs provide strong, almost overwhelming, evidence that some sources classified as QSOs are in the nuclei of spiral galaxies. There does remain the objection that sources in spirals are Seyfert I galaxies rather than "true" QSOs. However, HCCGM emphasized that they could not distinguish in any way between X-ray selected QSOs and traditional QSOs. The object 0241+622 is especially important, because it has the largest optical luminosity of the

29 QSOs observed by HCCGM. Even if 0241 + 622's reddening is as low as  $E(B-V) = 0.8$ , it is their most luminous source, and it is more luminous than many objects classified as QSOs.

The apparent discovery of spiral galaxies underlying some low-redshift QSOs strengthens the long-standing hypothesis that there is a continuum of properties between Seyfert I galaxies and the lower luminosity QSOs. In spite of this progress, there are still many unanswered questions about the relationship between a QSO and the host galaxy and its environment. Many of the most luminous quasars are symmetrical, triple radio sources, and are indistinguishable from the symmetrical triples produced in giant ellipticals. Hintzen, Ulvestad, and Owen (1983) found that  $\sim 45\%$  of quasars in the 3C, 4C, and Molonglo catalogs with  $z < 1.5$  are triple sources with well-defined radio axes. Further indirect evidence for an origin in elliptical galaxies comes through analogy with wide-angle radio-tailed ellipticals. Hintzen, Ulvestad, and Owen (1983) found that  $\sim 15\%$  of the quasar triples are bent by more than  $20^\circ$ , which suggests that the parent galaxies are orbiting in rich clusters containing a

relatively dense intracluster media. Although the data suggest that quasar radio triples are in elliptical galaxies, there is a possibility that spirals may have produced such sources in the past.

QSOs with  $z \leq 0.2$  are rarely found in rich clusters, but frequently in small groups (Stockton 1978, 1980). Miller (1981) studied nine low-luminosity QSOs with  $0.096 \leq z \leq 0.425$  and showed that they cannot be in first-ranked ellipticals. Phillips (1980) presented photographs and spectroscopy of the X-ray QSO MR 2251 - 178 which emphatically place it in a cluster of galaxies. Interestingly, even a casual inspection of Phillips's photographs shows that the slightly fuzzy QSO cannot be in either a giant elliptical or giant spiral. Clearly a great deal of work is yet to be done before we fully understand the where and why of QSOs.

We acknowledge the financial support of NSF grant AST 77-27745 and the Alfred P. Sloan Foundation and thank J. Miller and the KPNO staff for providing aperture plates.

#### REFERENCES

- Apparao, K. M. V., Bignami, G. F., Maraschi, L., Helmken, H., Margon, B., Hjellming, R., Bradt, H. V., and Dower, R. G. 1978, *Nature*, **273**, 450.  
 Boroson, T. 1981, *Ap. J. Suppl.*, **46**, 177.  
 Bothun, G. D., Romanishin, W., Margon, B., Schommer, R. A., and Chanan, G. A. 1982, *Ap. J.*, **257**, 40.  
 Ford, H. C. 1978, *Bull. AAS*, **10**, 450.  
 Grandi, S. A. 1982, *Ap. J.*, **255**, 25.  
 Hintzen, P., Ulvestad, J., and Owen, F. 1983, *A.J.*, **88**, 709.  
 Hutchings, J. B., Crampton, D., Campbell, B., Gower, A. C., and Morris, S. C. 1982, *Ap. J.*, **262**, 48 (HCCGM).  
 Justusson, B. I. 1981, in *Two-Dimensional Digital Signal Processing II*, ed. T. S. Huang (New York: Springer-Verlag).  
 Malkan, M. A., and Sargent, W. L. W. 1982, *Ap. J.*, **254**, 22.  
 Margon, B. M., and Kwitter, K. B. 1978, *Ap. J. (Letters)*, **224**, L43 (MK).  
 Miller, J. S. 1981, *Pub. A.S.P.*, **93**, 681.  
 Oke, J. B. 1974, *Ap. J. Suppl.*, **27**, 21.  
 Pence, W. 1976, *Ap. J.*, **203**, 39.  
 Peterson, B. A. 1970, *A.J.*, **75**, 695.  
 Phillips, M. M. 1980, *Ap. J. (Letters)*, **236**, L45.  
 Robinson, L. B., and Wampler, E. J. 1972, *Pub. A.S.P.*, **84**, 161.  
 ———. 1973, in *Astronomical Observations with Television Type Sensors*, ed. J. W. Gaspary and G. A. H. Walker (Vancouver: University of British Columbia), p. 69.  
 Romanishin, W. 1983, *M.N.R.A.S.*, **204**, 909.  
 Sandage, A. 1972, *Ap. J.*, **178**, 1.  
 Sparke, L. S., Kormendy, J., and Spinrad, H. 1980, *Ap. J.*, **235**, 755.  
 Spinrad, H. 1976, *Pub. A.S.P.*, **88**, 565.  
 Stockton, A. 1978, *Ap. J.*, **223**, 747.  
 ———. 1980, in *IAU Symposium 92, Objects at High Redshift*, ed. G. O. Abell and P. J. E. Peebles (Dordrecht: Reidel), p. 89.  
 Stone, R. P. S. 1974, *Ap. J.*, **193**, 135.  
 ———. 1977, *Ap. J.*, **218**, 767.  
 Strom, K. M., and Strom, S. E. 1978, *A.J.*, **83**, 73.  
 West, R. M., Danks, A. C., and Alcaïno, G. 1978, *Astr. Ap.*, **62**, L13.  
 Whitford, A. E. 1958, *A.J.*, **63**, 201.  
 Wilson, A. S., and Penston, M. V. 1979, *Ap. J.*, **232**, 389.

R. CIARDULLO and H. FORD: Space Telescope Science Institute, Homewood Campus, Baltimore, MD 21218

B. MARGON: Department of Astronomy, FM-20, University of Washington, Seattle, WA 98195

W. ROMANISHIN: Code 681, Goddard Space Flight Center, Greenbelt, MD 20771